ACS APPLIED POLYMER MATERIALS

pubs.acs.org/acsapm Article

Functional Poly(*p*-terphenyl-*co*-4-acetylpyridine) Membranes for High-Temperature Proton Exchange Membrane Fuel-Cell Applications

Tian Luan, Yaping Jin, Danni Wu, Wei Wei, Jingshuai Yang,* and Jin Wang*

Cite This: https://doi.org/10.1021/acsapm.4c04024 Read Online

ACCESS | Metrics & More | Article Recommendations

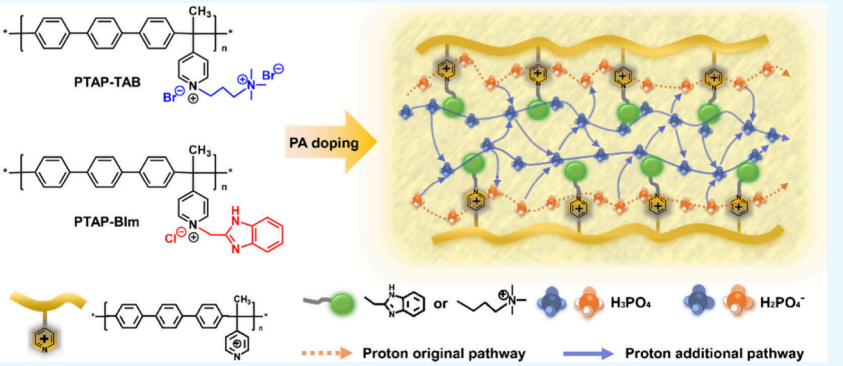

ABSTRACT: The development of high-temperature proton exchange membranes (HT-PEMs) with low cost, simple synthetic pathways, and superior physicochemical performance is of paramount importance for their successful integration into fuel cells. Herein, we prepare HT-PEMs by grafting alkaline side-chain groups onto poly(*p*-terphenyl-*co*-4-acetylpyridine) membranes (PTAP-*R*), taking 2-chloromethylbenzimidazole (BIm) and (3-bromopropyl)trimethylammonium bromide (TAB) as functionalized reagents. Initially, PTAP is synthesized via a straightforward Friedel−Crafts polymerization process. For the purpose of increasing the phosphoric acid (PA) doping content along with improving conductivity, BIm or TAB with alkaline side chains is incorporated onto the PTAP backbones. Comparative analysis reveals that the PTAP-BIm membrane accomplishes an exceptional PA doping level of 289%, and the conductivity attains 122 mS/cm at 180 °C in nonhumidification conditions. Large amounts of PA molecules provide numerous active sites for proton transfer, leading to the development of extensive and dynamic hydrogen bonding networks along with densely interconnected transport pathways, which offer additional pathways for effective proton conduction. Furthermore, the H_2-air fuel cell utilizing PTAP-BIm membrane with 289%PA achieves a peak power density of 324 mW/cm^2 at 160 °C without backpressure. This study elucidates a cost-effective and mild approach for fabricating high-performance HT-PEMs that hold great potential in HT-PEM fuel-cell applications.

KEYWORDS: *poly(p-terphenyl-co-4-acetylpyridine), alkaline side chain groups, proton transfer, high-temperature proton exchange membrane, fuel cell*

1. INTRODUCTION

Proton exchange membrane fuel cell (PEMFC) is a clean energy conversion device and exhibits low pollution, high conversion efficiency and power density, silent operation, as well as a broad range of applications, making it well concerned.[1,2] High-temperature PEMFCs (HT-PEMFCs) afford several additional advantages, namely, improved electrode reaction kinetics, simplified hydrothermal management system, and higher fuel impurities tolerance at elevated operating temperature (100−200 °C). These advantages greatly enhance the overall working efficiency of HT-PEMFC systems and effectively address challenges related to the storage and transportation of pure hydrogen fuel under low-temperature conditions.[3−5] The high-temperature proton exchange membrane (HT-PEM) serves as the key component in HT-PEMFCs by conducting proton and separating the fuel gas between two electrodes at elevated temperatures.[4,6] Alkaline polymer membranes doped with inorganic acids can conduct protons under anhydrous conditions. Phosphoric acid

Received: December 15, 2024
Revised: February 20, 2025
Accepted: February 20, 2025

(PA)-doped polybenzimidazole (PBI) has been broadly researched since they were first developed by Wainright et al.,[7] undergoing subsequent modifications.[5,6,8,9] Acid-doped PBI and its derivatives demonstrated outstanding proton conductivity, exceptional mechanical property as well as thermal stability in the operating environment of HT-PEMFCs.[10] Nevertheless, the further development can be limited as high-molecular-weight PBI polymers can be poorly soluble in polar solvents and exhibit a toxicity associated with monomer synthesis.[5,11] Consequently, materials possessing superior properties were developed and applied as membrane electrolytes for polymer membrane fuel-cell applications.

Poly(aryl ether) polymers have been extensively investigated due to their cost-effectiveness, excellent mechanical property, and adequate thermal stability. Moreover, the molecular structure of these polymers is highly designable and can be regulated through chemical modifications to obtain remarkable physicochemical properties. Various poly(aryl ether) polymers incorporating functional groups in their backbones have been reported for HT-PEMs, which have been further enhanced by optimizing the molecular architecture, adjusting the content of functional groups, synthesizing block copolymers, and employing chemical cross-linking techniques.[2,12,13] The structural design of HT-PEMs with diverse alkaline groups on the side links is more flexible. Introducing tertiary amine groups or nitrogen heterocyclic rings into aromatic polymers represents an alternative strategy for preparing HT-PEMs. These polymers can be modified with alkaline groups through halogenation substitution reactions and S_N2 nucleophilic substitution reactions, providing acid doping sites. For instance, imidazolium groups with various structures were grafted onto polysulfone (PSU),[11,14,15] while nitrogenous heterocyclic and tertiary amine groups were introduced on poly(ether ether ketone) or poly(aryl ether sulfone),[16,17] which exhibited excellent PA adsorption capacity and proton conductivities. However, the complex synthesis process involving hazardous reagents and uncertain grafting degree limited widespread development. Additionally, the aromatic ether bonds in the polymer matrix easily attacked free radicals, resulting in degradation of the membrane materials.

Polyaromatic polymers lacking aryl ether bonds or benzylic sites can be synthesized simply through the Friedel−Crafts acylation reaction, catalyzed by superacids under mild and facile conditions. Furthermore, these polymers exhibited a high degree of polymerization and exceptional thermal stability.[18,19] Jannasch's group developed a series of poly(arylene piperidinium)s used as anion exchange membranes, which were demonstrated outstanding conductivity and stability under alkaline solutions.[20] Subsequently, polyaromatic polymers have been widely used as membranes matrix in alkaline fuel cells,[21,22] water electrolysis,[23,24] vanadium redox flow battery,[25,26] and HT-PEMFCs.[27−30] Building upon polyaromatic polymers, extensive efforts have been invested in investigating the main chain structures of the polymers to enhance their physicochemical properties for fuel-cell applications. Chao et al. developed a range of membranes, as well as binder materials modified with different nitrogen-containing heterocyclic groups. Consequently, a peak power density based on TP-4-IM reached 1004 mW cm^{-2} at 200 °C when utilizing hydrogen and oxygen.[27] More recently, our group synthesized a range of pyridine-containing aromatic copolymers with different backbones incorporating rigid, flexible, or bulky moieties. Among them, the P(TP-*co*-DMF)/194%PA membrane containing 9,9-dimethylfluorene structures achieved the best comprehensive performance, and the peak power density reached 947 mW cm^{-2} as tested in hydrogen and oxygen fuel cells at 180 °C.[31] Incorporating side chain groups onto polymer backbones is a very effective way for enhancing physicochemical properties of membranes.[32,33] For instance, by introducing side chain groups into the PTP-C5/PA membrane structure, the PA uptake was increased and conductivity was significantly improved. Moreover, this proposed membrane revealed a peak power density of 676 mW cm^{-2} at 210 °C in hydrogen-air battery test without backpressure.[34]

Based on the previous studies,[29,33] the two alkaline side chain groups were grafted onto PTAP membranes through nucleophilic substitution in order to further enhance the acid doping content and conductivity in this work. Two different basic groups, namely, 2-chloromethylbenzimidazole (BIm) and (3-bromopropyl) trimethylammonium bromide (TAB), were introduced into the original polymer backbone containing pyridine to prepare HT-PEMs (referred to as PTAP-*R*). This not only increased the density of acid doping sites for proton transfer but also investigated the impact of different aliphatic amine or bulky *N*-heterocyclic group side-chain structures on membrane materials' physicochemical properties. Therefore, a more comprehensive study of the PTAP series membranes was conducted. The membrane performance and the fuel-cell property based on PTAP-*R* were assessed to investigate the fabricated membranes' technical feasibility in HT-PEMFCs application.

2. EXPERIMENTAL SECTION

2.1. Materials. Trifluoromethanesulfonic acid (TFSA), trifluoroacetic acid (TFA), *p*-terphenyl (TP), 2-chloromethylbenzimidazole (BIm), and (3-bromopropyl)trimethylammonium bromide (TAB) were came from Adamas Reagent. Meanwhile, 4-acetylpyridine (AP) was procured from Energy Chemical. *N*-methyl-2-pyrrolidone (NMP), dimethyl sulfoxide (DMSO), dichloromethane (CH_2Cl_2), diethyl ether, sodium bicarbonate ($NaHCO_3$), hydrogen peroxide (H_2O_2), and phosphoric acid were provided by Sinopharm Chemical Reagent. These chemicals were utilized directly.

2.2. Synthesis of Polymers. The PTAP was prepared through superelectrophilic activation, following previously reported methods.[29] TP (15.6 mmol) and AP (20.4 mmol) were dissolved in CH_2Cl_2 at a mole ratio of 1:1.3 under an ice bath. To adjust the solution's acidity, 0.8 mL of TFA was added subsequently. The polymerization reaction was initiated by the gradual addition of TFSA, with continuous mechanical stirring of the cooled solution. This reaction proceeded for 1 h under ice bath conditions and continued at RT for approximately 48 h, resulting in a dark blue, viscous solution. The final product was transferred to the 1 M $NaHCO_3$ solution, then a slight yellow hue precipitate formed. The PTAP product was extensively washed until it reached neutrality and then dried at 100 °C for 24 h. The inherent viscosity of PTAP was tested as 0.596 dL g^{-1} by using a PTAP/NMP solution (0.5 g dL^{-1}) at 25 °C with an Ubbelohde viscometer. After three testings for each sample, the viscosity was obtained from the formula $\eta = [\ln(t_c/t_0)]/c$. The parameters t_c and t_0 represents the polymer solution efflux times and NMP solvent efflux time, respectively, and c is 0.5 g dL^{-1}.

2.3. Preparation of Functionalized PTAP Membranes. The PTAP was functionalized with BIm and TAB through a nucleophilic substitution reaction, as depicted in Figure 1, resulting in the formation of cationic PTAP polymers with distinct alkaline side chains termed PTAP-BIm and PTAP-TAB, respectively. To illustrate the preparation process of the PTAP-TAB membrane in detail, TAB was initially added to a mixture of DMSO and NMP (1:3) under refluxing conditions at 80 °C with magnetic stirring until it was

https://doi.org/10.1021/acsapm.4c04024
ACS Appl. Polym. Mater. XXXX, XXX, XXX−XXX

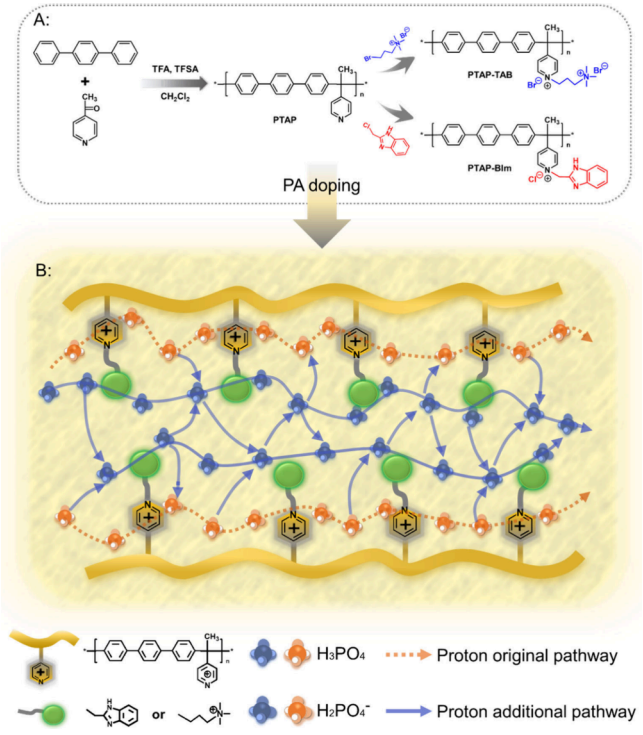

Figure 1. (A) Synthesis of the PTAP and functionalized PTAP-*R* polymers and (B) schematic of proton transport in the PA-doped PTAP-*R* membrane.

completely dissolved. Subsequently, the mixture of the aforementioned solution and NMP solution containing the PTAP polymer received 10 h of stirring at 80 °C to facilitate the grafting reaction. The resulting homogeneous solution underwent precipitation course in diethyl ether, and then was thoroughly cleaned and filtered before vacuum drying. A 2 wt % solution was formed for membranes preparation after the dissolution of the obtained product in DMSO. The solution was poured onto a Petri dish for 24 h of evaporation at 80 °C. Finally, the membranes were peeled off from dish, followed by a thorough wash using deionized water and another 48 h of drying at 50 °C to obtain homogeneous and transparent membranes with a thickness of 45 ± 5 μm (see Figure 3, presented later in this work).

2.4. Acid Doping and Swellings. The PA doping process involved immersing dry membranes in 75 and 85 wt % PA solutions at a temperature of 45 °C until equilibrium was achieved. After the removal of the excess PA on the sample surface using filter paper, the mass gains were taken into account for calculating the respective acid doping content (acid%), according to eq 1, and the dimensional alternation of the raw and acid-doped membranes was considered for calculating the area swelling (AS%) and volume swelling (VS%), using eqs 2 and 3. In the equations, m_0, S_0, V_0 and m, S, and V respectively denote the mass, area, and volume of initial and PA-doped samples.

$$\text{acid\%}\,(\%) = \frac{m - m_0}{m_0} \times 100\% \tag{1}$$

$$\text{AS\%}\,(\%) = \frac{S - S_0}{S_0} \times 100\% \tag{2}$$

$$\text{VS\%}\,(\%) = \frac{V - V_0}{V_0} \times 100\% \tag{3}$$

2.5. Characterizations. The ^{1}H NMR spectra of PTAP and PTAP-*R* membranes were acquired on a Bruker AVANCE 600 MHz spectrometer, utilizing a deuterated reagent ($CDCl_3$ and DMSO-d_6) as solvent. We collected the FT-IR spectra on a Thermo Fisher Scientific Nicolet iS20 instrument in the 4000−500 cm^{-1}. SEM analysis was employed to characterize the surface morphology of membranes by using a Model SU 8000 microscope after platinum coating. Their chemical stability was determined through a Fenton test, utilizing a solution containing 3.0 wt % H_2O_2, along with 4 ppm Fe^{2+} for a specified duration at 68 °C. After each exposure period, the collected samples were cleaned and then underwent drying treatment at 80 °C until their mass remained constant. Subsequently, the dried films were replaced into the refreshed Fenton solution, and this process was repeated to assess their chemical stability, based on mass loss and membrane integrity during the stability test. The thermogravimetric analysis (TGA) served for assessing the membranes' thermal stability under the assistance of a NETZSCH STA 449F5 instrument. We conducted TGA measurements at 30−800 °C within a nitrogen atmosphere. In this process, the heating rate is 10 °C/min. In addition, a tensile strength instrument (CMT200) was employed for evaluating the membrane mechanical properties, and the curves were collected under RT conditions when the stretching speed was set at 5 mm min^{-1}. Prior to testing, the membranes were made into dumbbell shapes according to the mold specifications, with a length of 25 mm and a width of 4 mm.

2.6. Proton Conductivity. We measured the proton conductivity by virtue of the four-probe technique at a frequency of 4 kHz.[35] For eliminating the influence of moisture, the membrane samples underwent 1 h of drying treatment at 100 °C before testing. Conductivity measurements were conducted from 100 to 180 °C in a nonhumidified environment. The conductivity values were calculated according to eq 4, where the σ and R denote conductivity and resistance, respectively, and l and S represent the distance between two electrodes and membrane's cross-sectional area.

$$\sigma = \frac{l}{R \times S} \tag{4}$$

2.7. Fuel Cell Tests. Membrane electrode assemblies (MEAs) were fabricated via a hot pressing process at 120 °C under 2 MPa pressure for 3 min. Following fabrication, the performance of fuel cell was evaluated to assess the application potential of the membranes prepared. Each MEA featured an active area of 1 cm^2, incorporating a Pt/C catalyst and PBI binder with loadings of 1.5 mg/cm^2 and 0.07 mg/cm^2. The single-cell performance evaluation employed hydrogen (80 mL/min) and air (200 mL/min) as reactants. The experiment process was conducted at temperatures spanning from 120 °C to 160 °C, without humidification or backpressure applied.

3. RESULTS AND DISCUSSION

3.1. PTAP-R Membrane Structures. ^{1}H NMR spectroscopy was employed to verify the chemical structures of PTAP, PTAP-TAB, and PTAP-BIm membranes, as illustrated in Figure 2A. For the PTAP spectrum, the methyl proton (H_1) exhibited a chemical shift at 2.24 ppm, while the pyridine ring H (peak 2 and peak 3) appeared at 7.13 and 8.55 ppm, respectively. The characteristic peaks among 7.20−7.67 ppm were ascribed to the H in the aromatic phenyl groups of polymer main chain, aligning with findings from prior studies.[36] Comparing with the characteristic signals of PTAP, following the introduction of TAB and BIm, the hydrogen peak (H_2 and H_3) associated with the pyridine ring moved to higher chemical shifts. This shift can primarily be attributed to the electron-withdrawing effect exerted by grafting side chains. Furthermore, the signals at 4.67 ppm (H_a) and 3.15 ppm (H_d) emerged due to the methylene linkage and terminal methyl groups $-N^+(CH_3)_3$ in PTAP-TAB.[37] Meanwhile, the peaks observed at 13.36 (H_f) and 7.00−7.40 ppm ($H_{g,h}$) were both corresponding to the grafted benzimidazole ring structure in PTAP-BIm.[17,38] Moreover, peak "e" in $-CH_2-$ of PTAP-BIm (δ = 6.25 ppm) was higher than that of the PTAP-TAB, possibly because of the more electrophilic activity of the imidazolum group.[39] Notably distinct characteristic signals were observed in both PTAP-TAB and PTAP-BIm NMR

https://doi.org/10.1021/acsapm.4c04024
ACS Appl. Polym. Mater. XXXX, XXX, XXX−XXX

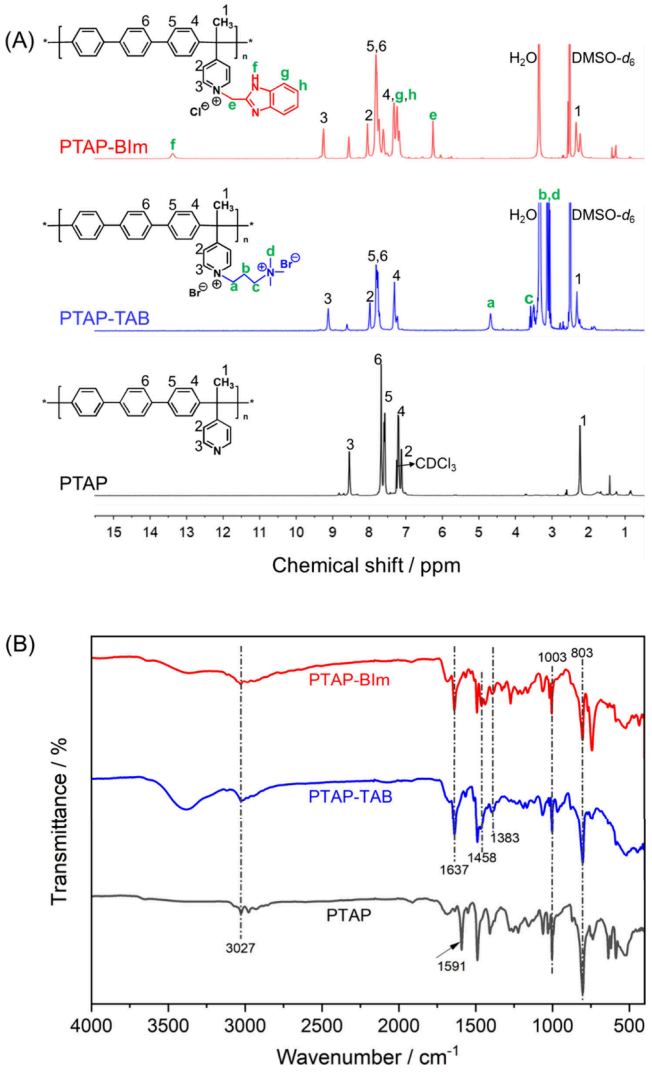

Figure 2. (A) ^{1}H NMR spectra and (B) FT-IR spectra of PTAP and its functionalized PTAP-*R* membranes.

spectra, confirming successful grafting onto the main chain. The grafting degrees of PTAP-TAB and PTAP-BIm were calculated as 97% and 92%, respectively, which was determined by integral area ratio of the methylene group ($H_{a/e}$) to pyridine ring (H_3).

In addition, we focused on examining membrane samples in terms of the chemical structure using FT-IR spectroscopy data. According to Figure 2B, the signal at 3027 cm^{-1} is indicative of the stretching vibrations of aromatic C−H. Meanwhile, the signals at 1006 and 796 cm^{-1} indicate the deformation vibrations of the C−H bonds.[29,31] The peak observed at 1591 cm^{-1} results from the C−N stretching vibration of pyridine rings in PTAP, which shifts to 1637 cm^{-1} in the PTAP-*R* membranes spectra. This phenomenon can be explained by the impact of quaternization on the pyridine ring conjugated structure.[37,40] Moreover, the bending vibration of methylene and stretching vibration of quaternary ammonium appears at 1458 and 1383 cm^{-1}, respectively.[37,41] Consequently, ^{1}H NMR and FT-IR analyses validate the chemical structures of all fabricated membranes.

Through a straightforward solution-casting method, membranes of PTAP, PTAP-TAB, and PTAP-BIm were prepared. In fuel-cell applications, the integrity of the membrane is essential for efficiently isolating the anode from the cathode. As depicted in Figure 3, the resulted membranes were uniform,

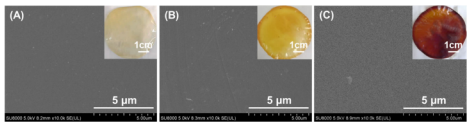

Figure 3. Surface morphologies by SEM and photographic images of (A) PTAP, (B) PTAP-TAB, and (C) PTAP-BIm membranes.

transparent, presenting a yellow or brown hue, and also exhibited excellent resilience. The surface morphologies images and photographs of the three membranes confirmed their dense and nonporous microstructures without phase separation, which were crucial for reducing gas crossover in MEAs and essential for fuel-cell applications.[31,33,42,43]

3.2. Chemical and Thermal Stabilities. The membrane is inevitably attacked by hydroxyl radicals and peroxyl (•OH and •OOH) when assembled in fuel cells.[44] Therefore, the chemical stability of HT-PEM is a key factor in evaluating membrane materials because it directly determines the battery's performance and service life. The chemical stability of PTAP, as well as its grafted membranes, was normally evaluated using Fenton's reagent. Figure 4A shows the mass retention rates of membrane samples during the chemical stability test over time. The inserted photos depict the appearance changes in the membrane materials before and after undergoing the oxidative test. The PTAP membrane still maintained its original shape with a mass retention rate of 86.4% at the end of this experiment. The PTAP-TAB membrane broke into fragments after 10 h Fenton test while the PTAP-BIm membrane remained relatively intact with crimp after being subjected to Fenton test for 234 h. These results indicated that grafting quaternary ammonium and imidazolium groups onto polymer main chains significantly influences the oxidative stability of the films.[11,33] The PTAP-BIm membrane exhibited better chemical stability, while the PTAP-TAB membrane was more vulnerable to free radical attack, leading to degradation due to its alkane chain. Consequently, considering comprehensive comparison results suggested that the PTAP-BIm membrane held more promise for fuel-cell applications.

Thermal stability is a critical attribute for evaluating membranes designed for HT-PEMs. As shown in the TGA curves in Figure 4B, PTAP and PTAP-*R* membranes exhibit good thermal stabilities until to 200 °C. At approximately 100 °C, the observed minor mass change does not exceed 1.5%, which is mainly because of the evaporation of absorbed moisture.[11] The breakdown of the grafted side-chain functional groups results in a reduction in weight near 300 °C,[33] while the subsequent mass reduction results from the polymer main chain decomposition. Thermogravimetric analysis indicates that these synthesized PTAP-*R* membranes demonstrate sufficient thermal stability under the working conditions of HT-PEMFCs.

3.3. Acid Doping and Swellings. The PTAP and PTAP-*R* membranes were doped in 75 and 85 wt % PA solution, respectively, and subsequently placed in a 45 °C oven until the membrane mass presented no more change. The PTAP membrane can absorb PA via interactions involving acid−base reactions and hydrogen bonding, because of the pyridine groups present within the polymer's repeating units. In

https://doi.org/10.1021/acsapm.4c04024
ACS Appl. Polym. Mater. XXXX, XXX, XXX−XXX

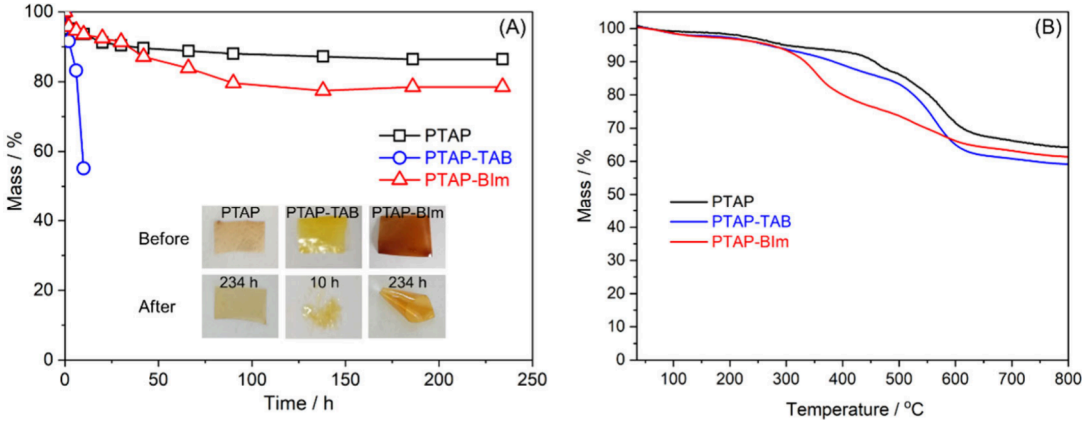

Figure 4. (A) Fenton test at 68 °C (reagent: 3 wt % H_2O_2, 4 ppm of Fe^{2+}) and (B) TGA curves in nitrogen gas of PTAP, PTAP-TAB, and PTAP-BIm membranes.

comparison with PTAP, the PA absorption was significantly increased for the PTAP-*R* membranes at different concentrations of PA solution, resulting from the attached alkaline groups in their side chains. It was observed that the acid percentage in the PTAP-BIm membrane exceeded that in the PTAP-TAB membrane when the membrane grafting degree was similar; i.e., PTAP-BIm soaked in 85 wt % PA displayed a highest acid doping content up to 289%, while under identical conditions, the acid% for PTAP-TAB membrane was only 246%. This difference could be attributed to the presence of benzimidazole group, which not only increased the interaction site of PA, but also generated more free volume within the membrane. The acid doping results illustrated that grafting alkaline side chain groups is an available method to increase the membranes acid doping content.

Higher doping levels of PA molecules were beneficial to the increase in anhydrous proton conductivity; however, the increased phosphoric acid doping resulted in larger swellings and reduced dimensional stability. As displayed in Figure 5, the membranes with higher acid doping content exhibited more area and volume swellings. For instance, the PTAP-TAB/246% membrane showed 73% area swelling and 115% volume swelling, while the PTAP-BIm/289% membrane had values of 92% and 138%, respectively. Furthermore, after immersion in an 85% PA solution, the PSF-Im-70/235.8%PA membrane,

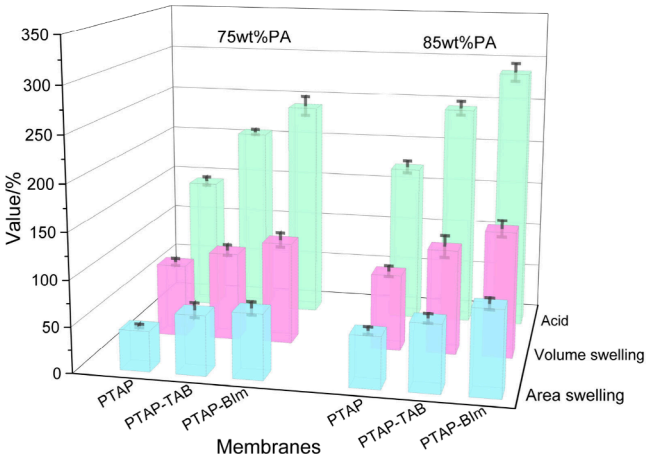

Figure 5. Acid percentage, area, and volume swellings of the membranes after immersed in different PA solutions.

poly(arylene ether sulfone) including pendent imidazole groups,[45] and (DAP-PSU-99)/235.90% membrane grafting with three tertiary amine groups onto polysulfone[14] experienced volume swellings of 194% and 155.15%, respectively. Compared to previously reported results, the PTAP-*R* membranes expressed better dimensional stability with a similar acid doping content, which was beneficial for promoting battery performance.

3.4. Mechanical Property. Long-term operation of fuel cells necessitates that HT-PEMs possess adequate mechanical stability to ensure consistent and reliable performance.[4,6] The PTAP and PTAP-*R* films tensile strength and elongation were investigated at room temperature after immersing them in PA solutions, as depicted in Figure 6. Generally, higher acid

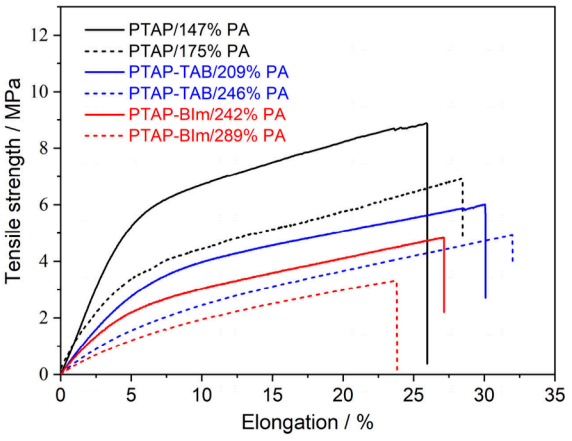

Figure 6. Tensile strength curves of PTAP and PTAP-*R* membranes immersed in 75 and 85 wt % PA solutions at RT.

doping content in membranes leads to lower tensile strength due to the reduced intermolecular forces caused by the plasticizing effect of phosphoric acid.[9,11] The tensile strength of the PTAP or PTAP-*R* membrane doped in 75 wt % PA was better than that of doped in 85 wt % PA. For instance, the tensile strength decreased from 4.8 MPa for PTAP-BIm/242% PA to 3.3 MPa for PTAP-BIm/289%PA, respectively. Although the tensile strength of PTAP-TAB/246%PA membrane was similar to that of PTAP-BIm/242%PA membrane, their elongation at break was different, probably resulting from the rigid structure in the PTAP-BIm membrane,

https://doi.org/10.1021/acsapm.4c04024
ACS Appl. Polym. Mater. XXXX, XXX, XXX−XXX

but the flexible alkyl side chain in the PTAP-TAB membranes. These results indicated that the mechanical properties were not only influenced by the plasticization of PA,[28] but also related to the structure of the polymer. It has been reported that the membrane is suitable for fuel cells when its tensile strength is greater than 1.5−2 MPa.[4,35] Therefore, the mechanical properties of the prepared PTAP-*R*/PA films could meet the requirements for assembling fuel cells.

3.5. Proton Conductivity. Figure 7 shows that the proton conductivities of all measured membranes increased as

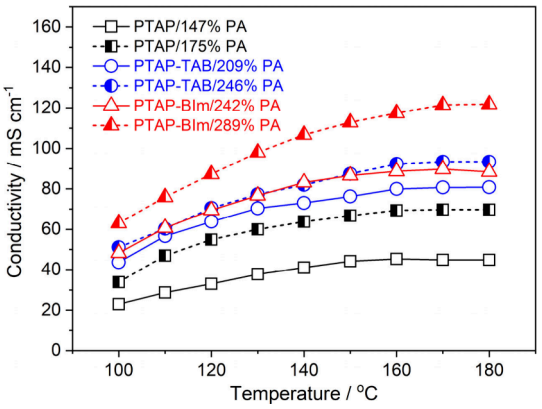

Figure 7. Conductivities of PA doped PTAP and PTAP-*R* membranes.

operating temperature elevated due to the enhanced proton mobility at high temperatures.[46] For example, at 100 to 180 °C, the conductivity of the PTAP-BIm/289%PA membrane elevated from 0.063 to 0.122 S cm^{-1}. As reported in the literature everywhere, higher levels of PA doping content resulted in greater proton conductivity. The anhydrous proton conductivity of PTAP-BIm/289%PA reached 0.122 S cm^{-1} at 180 °C, while the PTAP-TAB/246%PA membrane showed a value of 0.093 S cm^{-1} at the same temperature. A large number of PA molecules provided more active sites for proton transfer, promoting extensive dynamic hydrogen bonding networks and dense transport channels to be formed,[29] which offered additional proton pathways for proton conduction as illustrated schematically in Figure 1B. It should be noted that, while increasing PA uptake enhanced proton conductivity, it also compromised dimensional stability and mechanical strength, thereby affecting the membrane electrolyte durability in fuel cells. Therefore, addressing comprehensive requirements for both high proton conductivity and satisfactory mechanical stability continues to present a challenge, necessitating additional investigation.

3.6. Fuel-Cell Performance. With the objectives of validating whether the PA-doped PTAP-*R* membrane was technically feasible as a promising HT-PEM candidate, the MEA was assembled and the battery performance curves were measured. Fuel-cell tests based on the PTAP-BIm/289%PA membrane (63 μm in thickness) was carried out over temperatures from 120 to 160 °C in environments supplied with H_2 and air without humidification. As depicted in Figure 8, the open circuit voltage (OCV) is stable at approximately 0.90 V across the tested temperature range and did not exhibit a decrease with increasing temperature, indicating the low gas crossover through the membranes that hindered the gas fuels effectively.[34,42,43] The performance of the MEA exhibited

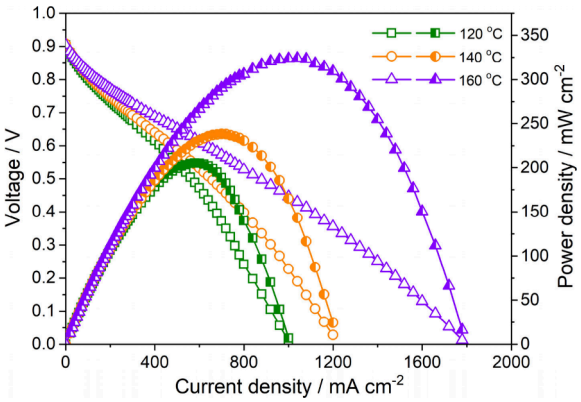

Figure 8. Fuel-cell performance based on the PTAP-BIm/289% PA membrane fueling with H_2 and air at 120−160 °C without humidification and back pressure.

substantial improvement at higher temperatures, ascribed to the accelerated proton transfer and enhanced electrode kinetics resulting from elevated operating temperatures.[1,47] The peak power density reached 324 mW cm^{-2} at 160 °C, but it was only 205 mW cm^{-2} at 120 °C. Compared with the results in the literature, the PTAP-BIm/289%PA membrane exhibited comparable performance in HT-PEMs. For instance, the PTP−PMIm membrane featured the long side-chain imidazole-based ionic liquid-based fuel cell achieved a peak power density of 318 mW cm^{-2} at 160 °C in an unhumidified hydrogen and air atmosphere.[35] The performance comparison of hydrogen-air fuel cells using various polymer membrane electrolytes at 160 °C is summarized in Table 1. It is evident that PTAP-BIm/289%PA showed better fuel-cell performance among the investigated membranes. It should be remarked that further optimization on fuel-cell testing should be done, including the test system, MEAs fabrication, hot-pressing procedure, electrodes and operating condition to improve the battery performance. Fuel-cell tests were regarded as an initial indication of the membrane applications feasibility and the test results based on PA doped PTAP-BIm membrane demonstrated its technical feasibility for HT-PEMFC applications.

4. CONCLUSION

Ether-free PTAP with alkaline side chain groups were fabricated using 2-chloromethylbenzimidazole (BIm) and (3-bromopropyl) trimethylammonium bromide (TAB) as functionalized reagents. PTAP was prepared via Friedel−Crafts polymerization at first. ^{1}H NMR results confirmed that PTAP was synthesized as well and BIm and TAB were grafted onto the polymer backbones successfully. SEM images and membrane photographs showed that the PTAP-*R* membranes were uniform and dense. The membrane properties were influenced by the molecular structure of the side chains groups, with Fenton testing demonstrating better chemical stability for PTAP-BIm compared to PTAP-TAB membrane. Incorporating alkaline side chain groups led to gradual increases in PA doping content and proton conductivity, resulting in excellent comprehensive properties for the PTAP-BIm membrane, which achieved a high acid doping content, i.e., 289%, and a remarkable conductivity of 122 mS/cm at 180 °C while possessing an acceptable tensile strength of 3.3 MPa. The membrane which contained a large number of PA molecules provided more active sites for proton conduction. As a result, extensive dynamic hydrogen bond networks as well as dense

https://doi.org/10.1021/acsapm.4c04024
ACS Appl. Polym. Mater. XXXX, XXX, XXX−XXX

Table 1. Comparisons of the Physicochemical Properties and H_2−Air Single Cell Performance at 160 °C of Acid-Doped Membranes

	Physicochemical properties				
Membrane	Acid% [%]	σ [S cm^{-1}] (T [°C])	Mechanical strength [MPa]	Power density [mW cm^{-2}]	ref
PTAP-BIm	289	0.117 (160)	3.3	324	This work
PTP−PMIm	323	0.138 (180)	4.5	318	35
QOPBI-15	167	0.049 (160)	27.0	260	44
PTP-C5	202	0.096 (180)	4.6	316	34
PPT	160	0.096 (180)	12.0	487[a]	30
PBI-Ben (15)	356	0.122 (180)	8.80	<225	48
$PAEK_{41}$-85%VIm	233	0.117 (180)	7.2	<250	49
QA50	387	0.085 (160)	7.1	584[b]	50

[a]Cathode: 0.15 MPa backpressure. [b]200 kPa backpressure.

proton channels would be formed within the membranes, offering additional pathways for proton transfer. The hydrogen−air single cell assembled with a PTAP-BIm/289%PA membrane exhibited a peak power density of 324 mW/cm^2 at 160 °C without backpressure or humidification. Our present work provided a low-cost and easy-to-operate synthesis route for preparing high-performance HT-PEMs, and the proposed membrane was expected for fuel-cell applications.

AUTHOR INFORMATION

Corresponding Authors

Jingshuai Yang − *Department of Chemistry, College of Sciences, Northeastern University, Shenyang 110819, China*; orcid.org/0000-0002-0275-0978; Email: yjs@mail.neu.edu.cn

Jin Wang − *School of Pharmacy, Shenyang Medical College, Shenyang 110034, China*; Email: wangjin@symc.edu.cn

Authors

Tian Luan − *School of Pharmacy, Shenyang Medical College, Shenyang 110034, China*

Yaping Jin − *Department of Chemistry, College of Sciences, Northeastern University, Shenyang 110819, China*

Danni Wu − *School of Pharmacy, Shenyang Medical College, Shenyang 110034, China*

Wei Wei − *Institute of Metal Research, Chinese Academy of Sciences, Shenyang 110016, China*

Complete contact information is available at: https://pubs.acs.org/10.1021/acsapm.4c04024

Author Contributions

All authors collaboratively made contributions to this manuscript.

Notes

The authors declare no competing financial interest.

ACKNOWLEDGMENTS

We sincerely acknowledge the Natural Science Foundation of China (Nos. 52403273, 51603031), the PhD Start-up Foundation of Liaoning Province (No. 2022-BS-341), and the Student Training Project of Shenyang Medical College (No. 20249072).

REFERENCES

(1) Haider, R.; Wen, Y.; Ma, Z.-F.; Wilkinson, D. P.; Zhang, L.; Yuan, X.; Song, S.; Zhang, J. High temperature proton exchange membrane fuel cells: progress in advanced materials and key technologies. *Chem. Soc. Rev.* **2021**, *50* (2), 1138−1187.

(2) Liu, R.; Wang, J.; Che, X.; Wang, T.; Aili, D.; Li, Q.; Yang, J. Facile synthesis and properties of poly(ether ketone cardo)s bearing heterocycle groups for high temperature polymer electrolyte membrane fuel cells. *J. Membr. Sci.* **2021**, *636*, No. 119584.

(3) Shi, N.; Wang, G.; Wang, Q.; Wang, L.; Li, Q.; Yang, J. Acid doped branched poly(biphenyl pyridine) membranes for high temperature proton exchange membrane fuel cells and vanadium redox flow batteries. *Chem. Eng. J.* **2024**, *489*, No. 151121.

(4) You, X.; Ju, Q.; Ma, Y.; Yi, G.; Jiang, Z.; Li, N.; Zhang, Q. High conductivity poly(meta-terphenyl alkylene)s proton exchange membranes for high temperature fuel cell. *Chem. Eng. J.* **2024**, *487*, No. 150535.

(5) Qu, E.; Hao, X.; Xiao, M.; Han, D.; Huang, S.; Huang, Z.; Wang, S.; Meng, Y. Proton exchange membranes for high temperature proton exchange membrane fuel cells: Challenges and perspectives. *J. Power Sources* **2022**, *533*, No. 231386.

(6) Peng, J.; Wang, S.; Fu, X.; Luo, J.; Wang, L.; Peng, X. Achieving over 1,000 Mw cm^{-2} power density based on locally high-density cross-linked polybenzimidazole membrane containing pillar[5]arene bearing multiple alkyl bromide as a cross-linker. *Adv. Funct. Mater.* **2023**, *33* (6), No. 2212464.

(7) Wainright, J.; Wang, J.; Weng, D.; Savinell, R.; Litt, M. Acid-doped polybenzimidazoles: a new polymer electrolyte. *J. Electrochem. Soc.* **1995**, *142* (7), L121−L123.

(8) Aili, D.; Yang, J.; Jankova, K.; Henkensmeier, D.; Li, Q. From polybenzimidazoles to polybenzimidazoliums and polybenzimidazolides. *J. Mater. Chem. A* **2020**, *8* (26), 12854−12886.

(9) Li, X.; Ma, H.; Wang, P.; Liu, Z.; Peng, J.; Hu, W.; Jiang, Z.; Liu, B.; Guiver, M. D. Highly conductive and mechanically stable imidazole-rich cross-linked networks for high-temperature proton exchange membrane fuel cells. *Chem. Mater.* **2020**, *32* (3), 1182−1191.

(10) Seselj, N.; Aili, D.; Celenk, S.; Cleemann, L. N.; Hjuler, H. A.; Jensen, J. O.; Azizi, K.; Li, Q. Performance degradation and mitigation of high temperature polybenzimidazole-based polymer electrolyte membrane fuel cells. *Chem. Soc. Rev.* **2023**, *52* (12), 4046−4070.

(11) Yang, J.; Wang, J.; Liu, C.; Gao, L.; Xu, Y.; Che, Q.; He, R. Influences of the structure of imidazolium pendants on the properties of polysulfone-based high temperature proton conducting membranes. *J. Membr. Sci.* **2015**, *493*, 80−87.

(12) Papadimitriou, K. D.; Paloukis, F.; Neophytides, S. G.; Kallitsis, J. K. Cross-linking of side chain unsaturated aromatic polyethers for high temperature polymer electrolyte membrane fuel cell applications. *Macromolecules* **2011**, *44* (12), 4942−4951.

(13) Charalampopoulos, C.; Kallitsis, K. J.; Anastasopoulos, C.; Daletou, M. K.; Neophytides, S. G.; Andreopoulou, A. K.; Kallitsis, J. K. Crosslinked polymer electrolytes of high pyridine contents for HT-PEM fuel cells. *Int. J. Hydrogen Energy* **2020**, *45* (60), 35053−35063.

(14) Zhang, J.; Zhang, J.; Bai, H.; Tan, Q.; Wang, H.; He, B.; Xiang, Y.; Lu, S. A new high temperature polymer electrolyte membrane based on tri-functional group grafted polysulfone for fuel cell application. *J. Membr. Sci.* **2019**, *572*, 496−503.

(15) Bai, H.; Wang, H.; Zhang, J.; Zhang, J.; Lu, S.; Xiang, Y. High temperature polymer electrolyte membrane achieved by grafting poly(1-vinylimidazole) on polysulfone for fuel cells application. *J. Membr. Sci.* **2019**, *592*, No. 117395.
(16) Zhang, N.; Wang, B.; Zhao, C.; Wang, S.; Zhang, Y.; Bu, F.; Cui, Y.; Li, X.; Na, H. Quaternized poly (ether ether ketone)s doped with phosphoric acid for high-temperature polymer electrolyte membrane fuel cells. *J. Mater. Chem. A* **2014**, *2* (34), 13996−14003.
(17) Wang, J.; Dai, Y.; Wan, R.; Wei, W.; Xu, S.; Zhai, F.; He, R. Grafting free radical scavengers onto polyarylethersulfone backbones for superior chemical stability of high temperature polymer membrane electrolytes. *Chem. Eng. J.* **2021**, *413*, No. 127541.
(18) Diaz, A. M.; Zolotukhin, M. G.; Fomine, S.; Salcedo, R.; Manero, O.; Cedillo, G.; Velasco, V. M.; Guzman, M. T.; Fritsch, D.; Khalizov, A. F. A novel, one-pot synthesis of novel 3F, 5F, and 8F aromatic polymers. *Macromol. Rapid Commun.* **2007**, *28* (2), 183−187.
(19) Park, E. J.; Kim, Y. S. Quaternized aryl ether-free polyaromatics for alkaline membrane fuel cells: synthesis, properties, and performance - a topical review. *J. Mater. Chem. A* **2018**, *6* (32), 15456−15477.
(20) Olsson, J. S.; Pham, T. H.; Jannasch, P. Poly(arylene piperidinium) hydroxide ion exchange membranes: synthesis, alkaline stability, and conductivity. *Adv. Funct. Mater.* **2018**, *28* (2), No. 1702758.
(21) Liu, M.; Hu, X.; Hu, B.; Liu, L.; Li, N. Soluble poly(aryl piperidinium) with extended aromatic segments as anion exchange membranes for alkaline fuel cells and water electrolysis. *J. Membr. Sci.* **2022**, *642*, No. 119966.
(22) Wang, X.; Qiao, X.; Liu, S.; Liu, L.; Li, N. Poly(terphenyl piperidinium) containing hydrophilic crown ether units in main chains as anion exchange membranes for alkaline fuel cells and water electrolysers. *J. Membr. Sci.* **2022**, *653*, No. 120558.
(23) Wang, Q.; Wei, T.; Peng, Z.; Zhao, Y.; Jannasch, P.; Yang, J. High-performance anion exchange membranes based on poly(oxindole benzofuran dibenzo-18-crown-6)s functionalized with hydroxyl and quaternary ammonium groups for alkaline water electrolysis. *J. Colloid Interface Sci.* **2025**, *686*, 304−317.
(24) Chen, Q.; Huang, Y.; Hu, X.; Hu, B.; Liu, M.; Bi, J.; Liu, L.; Li, N. A novel ion-solvating polymer electrolyte based on imidazole-containing polymers for alkaline water electrolysis. *J. Membr. Sci.* **2023**, *668*, No. 121186.
(25) Mu, T.; Tang, W.; Shi, N.; Wang, G.; Wang, T.; Wang, T.; Yang, J. Novel ether-free membranes based on poly(p-terphenylene methylimidazole) for vanadium redox flow battery applications. *J. Membr. Sci.* **2022**, *659*, No. 120793.
(26) Wang, Q.; Zhang, Z.; Lv, P.; Peng, Z.; Yang, J. Poly(terphenyl pyridine) based amphoteric and anion exchange membranes with high ionic selectivity for vanadium redox flow batteries. *Chem. Eng. J.* **2025**, *505*, No. 158922.
(27) Chao, G.; Tang, H.; Li, R.; Ju, Q.; Guo, T.; Gao, H.; Lv, Z.; Niu, C.; Geng, K.; Li, N. Nitrogen heterocyclic polymers with different acidophilic properties as proton exchange membranes and binders for high-temperature fuel cells. *J. Membr. Sci.* **2024**, *692*, No. 122297.
(28) Ju, Q.; Tang, H.; Chao, G.; Guo, T.; Geng, K.; Li, N. Performance and stability of ether-free high temperature proton exchange membranes with tunable pendent imidazolium groups. *J. Mater. Chem. A* **2022**, *10* (47), 25295−25306.
(29) Jin, Y.; Wang, T.; Che, X.; Dong, J.; Li, Q.; Yang, J. Poly(arylene pyridine)s: New alternative materials for high temperature polymer electrolyte fuel cells. *J. Power Sources* **2022**, *526*, No. 231131.
(30) Bai, H.; Peng, H.; Xiang, Y.; Zhang, J.; Wang, H.; Lu, S.; Zhuang, L. Poly(arylene piperidine)s with phosphoric acid doping as high temperature polymer electrolyte membrane for durable, high-performance fuel cells. *J. Power Sources* **2019**, *443*, No. 227219.
(31) Lv, R.; Jin, S.; Li, L.; Wang, Q.; Wang, L.; Wang, J.; Yang, J. The influence of comonomer structure on properties of poly(aromatic pyridine) copolymer membranes for HT-PEMFCs. *J. Membr. Sci.* **2024**, *701*, No. 122703.
(32) Li, J.; Yang, C.; Zhang, X.; Xia, Z.; Wang, S.; Yu, S.; Sun, G. Alkyl-substituted poly(arylene piperidinium) membranes enhancing the performance of high-temperature polymer electrolyte membrane fuel cells. *J. Mater. Chem. A* **2023**, *11* (34), 18409−18418.
(33) Jin, Y.; Wang, T.; Che, X.; Dong, J.; Liu, R.; Yang, J. New high-performance bulky N-heterocyclic group functionalized poly(terphenyl piperidinium) membranes for HT-PEMFC applications. *J. Membr. Sci.* **2022**, *641*, No. 119884.
(34) Che, X.; Wang, L.; Wang, T.; Dong, J.; Yang, J. The effect of grafted alkyl side chains on the properties of poly(terphenyl piperidinium) based high temperature proton exchange membranes. *Ind. Chem. Mater.* **2023**, *1* (4), 516−525.
(35) Jin, Y.; Che, X.; Xu, Y.; Dong, J.; Pan, C.; Aili, D.; Li, Q.; Yang, J. An imidazolium type ionic liquid functionalized ether-free poly(terphenyl piperidinium) membrane for high temperature polymer electrolyte membrane fuel cell applications. *J. Electrochem. Soc.* **2022**, *169* (2), No. 024504.
(36) Li, Y.; Xu, S.; Wang, J.; Liu, X.; Yang, Y.; Yang, F.; He, R. Terphenyl pyridine based polymers for superior conductivity and excellent chemical stability of high temperature proton exchange membranes. *Eur. Polym. J.* **2022**, *173*, No. 111295.
(37) Xu, S.; Wu, W.; Wan, R.; Wei, W.; Li, Y.; Wang, J.; Sun, X.; He, R. Tailoring the molecular structure of pyridine-based polymers for enhancing performance of anion exchange electrolyte membranes. *Renewable Energy* **2022**, *194*, 366−377.
(38) Yang, J.; Aili, D.; Li, Q.; Xu, Y.; Liu, P.; Che, Q.; Jensen, J. O.; Bjerrum, N. J.; He, R. Benzimidazole grafted polybenzimidazoles for proton exchange membrane fuel cells. *Polym. Chem.* **2013**, *4* (17), 4768−4775.
(39) Yang, J.; Li, Q.; Jensen, J. O.; Pan, C.; Cleemann, L. N.; Bjerrum, N. J.; He, R. Phosphoric acid doped imidazolium polysulfone membranes for high temperature proton exchange membrane fuel cells. *J. Power Sources* **2012**, *205*, 114−121.
(40) Fang, J.; Wu, Y.; Zhang, Y.; Lyu, M.; Zhao, J. Novel anion exchange membranes based on pyridinium groups and fluoroacrylate for alkaline anion exchange membrane fuel cells. *Int. J. Hydrogen Energy* **2015**, *40* (36), 12392−12399.
(41) Zhang, D.; Xu, S.; Wan, R.; Yang, Y.; He, R. Functionalized graphene oxide cross-linked poly(2,6-dimethyl-1,4-phenylene oxide)-based anion exchange membranes with superior ionic conductivity. *J. Power Sources* **2022**, *517*, No. 230720.
(42) Ji, J.; Li, H.; Wang, W.; Li, J.; Zhang, W.; Li, K.; Yang, T.; Jin, W.; Tang, Y.; Li, W.; et al. Silane-crosslinked polybenzimidazole with different hydroxyl content for high-temperature proton exchange membrane. *J. Membr. Sci.* **2024**, *694*, No. 122423.
(43) Hu, X.; Ao, Y.; Gao, Y.; Liu, B.; Zhao, C. Facile preparation of triazole-functionalized poly(arylene perfluorophenyl) high temperature proton exchange membranes via para-fluoro-thiol click reaction with high radical resistance. *J. Membr. Sci.* **2023**, *687*, No. 122102.
(44) Hu, M.; Li, T.; Neelakandan, S.; Wang, L.; Chen, Y. Cross-linked polybenzimidazoles containing hyperbranched cross-linkers and quaternary ammoniums as high-temperature proton exchange membranes: Enhanced stability and conductivity. *J. Membr. Sci.* **2020**, *593*, No. 117435.
(45) Wang, J.; Zheng, J.; Zhao, Z.; Zhang, S. Synthesis and characterization of a novel poly(arylene ether sulfone) containing pendent imidazole groups for high temperature proton exchange membranes. *J. Mater. Chem.* **2012**, *22* (42), 22706−22712.
(46) Wang, J.; Liu, G.; Wang, A.; Ji, W.; Zhang, L.; Zhang, T.; Li, J.; Pan, H.; Tang, H.; Zhang, H. Novel N-alkylation synthetic strategy of imidazolium cations grafted polybenzimidazole for high temperature proton exchange membrane fuel cells. *J. Membr. Sci.* **2023**, *669*, No. 121332.
(47) Wang, X.; Wang, S.; Liu, C.; Li, J.; Liu, F.; Tian, X.; Chen, H.; Mao, T.; Xu, J.; Wang, Z. Cage-like cross-linked membranes with excellent ionic liquid retention and elevated proton conductivity for HT-PEMFCs. *Electrochim. Acta* **2018**, *283*, 691−698.

https://doi.org/10.1021/acsapm.4c04024
ACS Appl. Polym. Mater. XXXX, XXX, XXX−XXX

(48) Duan, C.; Luo, H.; Li, J.; Liu, C. A novel strategy to construct polybenzimidazole linked crosslinking networks for polymer electrolyte fuel cell applications. *Polymer* **2020**, *201*, No. 122555.
(49) Yang, J.; Jiang, H.; Wang, J.; Xu, Y.; Pan, C.; Li, Q.; He, R. Dual cross-linked polymer electrolyte membranes based on poly(aryl ether ketone) and poly(styrene-vinylimidazole-divinylbenzene) for high temperature proton exchange membrane fuel cells. *J. Power Sources* **2020**, *480*, No. 228859.
(50) He, D.; Liu, G.; Wang, A.; Ji, W.; Wu, J.; Tang, H.; Lin, W.; Zhang, T.; Zhang, H. Alkali-free quaternized polybenzimidazole membranes with high phosphoric acid retention ability for high temperature proton exchange membrane fuel cells. *J. Membr. Sci.* **2022**, *650*, No. 120442.

https://doi.org/10.1021/acsapm.4c04024
ACS Appl. Polym. Mater. XXXX, XXX, XXX−XXX